*Int. J. Heat Mass Transfer.* Vol. 34, No. 1, pp. 149–157, 1991
Printed in Great Britain

0017-9310/91 $3.00+0.00
Pergamon Press plc

# Bubble induced entrainment between stratified liquid layers

G. ALANSON GREENE,† JOHN C. CHEN‡ and MICHAEL T. CONLIN†

†Department of Nuclear Energy, Brookhaven National Laboratory, Upton, NY 11973, U.S.A.
‡Department of Chemical Engineering, Lehigh University, Bethlehem, PA 18015, U.S.A.

(*Received* 29 *September* 1989 *and in final form* 1 *March* 1990)

**Abstract**—The phenomenon of liquid entrainment by a gas bubble rising vertically across the interface between two immiscible liquid layers is addressed primarily by experiment. An analytical/empirical model is developed which predicts the volume of liquid entrained as a function of the bubble volume and the physical and transport properties of the two liquids. The entrainment efficiency is presented as a function of the reduced bubble volume and bubble Reynolds numbers in each fluid. When compared to the experimental data for eight immiscible liquid pairs, the correlation and the data exhibit good agreement.

## INTRODUCTION

### *Physical phenomenon and application*

CONSIDER the case of two immiscible liquids in stratified layers, as illustrated in Fig. 1. It is known that gas bubbles of sufficient size rising through the stratified layers can entrain some volume of the denser liquid from the lower layer into the upper layer of lighter liquid. This entrainment phenomenon has significant effects on both heat and mass transfer between the two liquid layers [1, 2]. This situation is encountered and is of concern in a number of applications. In chemical processing, gas bubbles are sometimes sparged into pools of stratified liquids in order to induce mixing and interface transport. In nuclear reactor safety, one is sometimes concerned with the possibility of stratified pools of molten fuel and metals through which flow bubbles of non-condensable gas arising from concrete decomposition below the liquid pools. In metallurgical processing, bubbles of oxygen, $SO_2$, and other gases may bubble through pools of molten metal with overlying pools of molten silica slag.

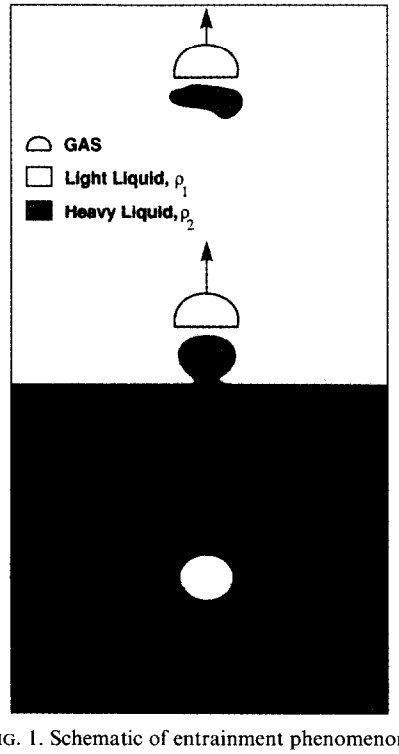


FIG. 1. Schematic of entrainment phenomenon.

In an earlier paper [3], it was shown that discrete gas bubbles must exceed a certain minimum volume to cause entrainment of the denser liquid into the upper pool; a theoretical criterion was developed to predict this onset condition. The objective of the present investigation is to determine the volume of the denser fluid that will be entrained by a discrete bubble, once this onset criterion is exceeded. The study is limited to that regime of gas flux which results in bubbly flow. Higher gas fluxes would lead to alternate flow regimes (e.g. churn turbulent flow) which may have very different mechanisms for fluid mixing between the two immiscible liquids.

### *Prior work*

Previous investigations reported in the literature indicate that entrainment between overlying immiscible liquid layers by bubbling gas is clearly observed for some fluid systems while apparently not observed for other fluids. Szekely [1] and Greene and Irvine [2] reported studies of liquid systems which did not support entrainment, but rather remained stratified. Szekely [1] presented a theoretical analysis of transient heat transfer at the interface by the surface renewal principles, while Greene and Irvine [2] presented experimental results for interfacial heat transfer and a dimensionless correlation of their data.

Mercier *et al.* [4] reported on visual observations in which a minimum bubble volume threshold was

## NOMENCLATURE

| | |
|---|---|
| $a$ | constant in equation (8) |
| $b$ | constant in equation (8) |
| $c$ | constant in equation (8) |
| $d_b$ | bubble diameter |
| $g$ | gravitational acceleration |
| $K$ | constant in equation (8) |
| $Re$ | Reynolds number |
| $u$ | velocity |
| $V$ | volume |
| $V_{go}$ | entrainment onset bubble volume. |

Greek symbols

| | |
|---|---|
| $\varepsilon$ | entrainment efficiency |
| $\mu$ | dynamic viscosity |
| $\rho$ | density |
| $\sigma_{12}$ | interfacial tension |
| $\phi$ | excess bubble volume. |

Subscripts

| | |
|---|---|
| b | bubble |
| e | entrainment |
| g | gas |
| m | maximum |
| 1 | light liquid |
| 2 | heavy liquid. |

observed (0.020 $cm^3$) for onset of entrainment between water and a variety of mineral oils. A similar observation was reported by Mori *et al.* [5] who observed a minimum bubble volume for penetration of an aqueous glycerol–R113 interface; for bubbles larger than this penetration threshold value (0.020–0.045 $cm^3$), entrainment of the lower fluid always occurred and increased with increasing bubble volume. Epstein *et al.* [6] reported on the onset of mixing and stratification in bubbling systems; they suggested that it is only necessary to know the mixture density to predict the pool configuration. In a similar study, however, Suter and Yadigaroglu [7] developed an entrainment criterion on the basis of stability considerations which include density and interfacial and surface tensions. Greene *et al.* [3] presented a theoretical and experimental study of entrainment in which both a bubble penetration threshold and an entrainment onset threshold were reported. The model is a function of the densities of the gas and two liquids, the interfacial tension between the liquids and the bubble volume; entrainment onset data for eight separate fluid pairs were found to be in good agreement with the entrainment onset criterion. The bubble penetration criterion was in agreement with the experimental observations of Mori *et al.* [5].

That the rate of entrainment between immiscible liquid layers increased with increasing bubble volume for a particular pair of fluids was reported by Poggi *et al.* [8], Cheung *et al.* [9], Veeraburus and Philbrook [10], and Mori *et al.* [5]. Mori *et al.* [5] presented data for glycerol–R113 which demonstrate an increase in entrained volume with an increase in bubble volume and a decrease in the viscosity of the light liquid. Entrainment mechanisms of film and bubble transport were observed by Poggi *et al.* [8], Veeraburus and Philbrook [10], and Mori *et al.* [5]. Cheung *et al.* [9] observed that entrainment could be affected by non-uniform gas bubbling. Although no model for the rate of entrainment is presented, Gonzalez and Corradini [11] reported experimental results for entrainment onset and emulsification for several fluid pairs as a function of the superficial gas velocity.

Heat transfer between overlying liquids both with and without entrainment was reported in refs. [2, 12–14]. It was observed that pools could be stratified, mixed, or homogenized depending upon the fluid properties and volumetric gas flux. The component of heat flux due to entrainment was observed to substantially increase the interlayer heat transfer over the stratified situation. A model for calculating the entrainment heat transfer as a combination of the stratified component and that due to direct mass transfer was presented in ref. [13]. The analysis requires a model for the rate of mass entrainment which, until now, was not available. It should be noted that Suo-Anttila [15] recently proposed a framework for calculating entrainment and entrainment heat transfer between overlying liquids with gas bubbling. However, models for the various processes involved are not offered.

### *Scope*

In the present investigation, experiments were conducted which permitted visual recordings of the entrainment process as well as quantitative measurements of the entrained liquid volumes. Studies of the visual records gave indications of the mechanisms involved in the entrainment process and guided the development of a semi-empirical correlation for prediction of the entrainment volumes. Additional experiments were carried out to measure a number of pertinent physical and transport properties required for the correlation model.

## EXPERIMENT

In order to investigate the phenomenon of bubble-induced entrainment between stratified liquids, the experimental investigation to be described was initiated. In this section we will discuss in detail the experimental apparatus and the experimental pro-

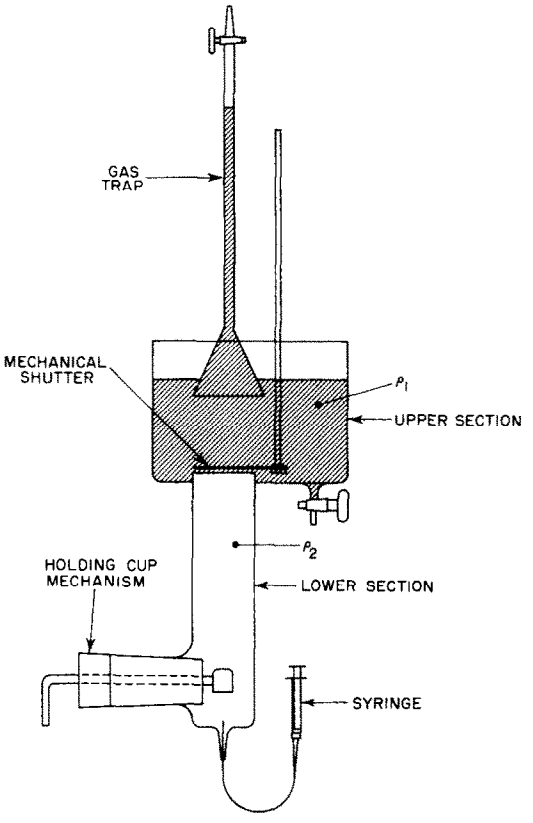


FIG. 2. Experimental apparatus.

cedure. It became necessary during this investigation to measure the physical and transport properties of the fluids that were used, as well as the bubble rise velocities for each of the fluids. These measurements will be discussed as well.

*Apparatus*

The experimental apparatus is illustrated in Fig. 2. It consisted of a vertical glass column having two cylindrical sections, and installed with devices for injecting and measuring gas bubbles of precise volumes and for collection of the entrained liquid volume. The denser and lighter fluids were contained in the lower and upper sections of the glass column, respectively. Two test columns were constructed for the entrainment experiments, a small column and a larger column. The dimensions of the upper and lower sections of the small column were 15.2 cm i.d. × 14.0 cm length and 5.0 cm i.d. × 23.5 cm length, respectively; the corresponding dimensions for the upper and lower sections of the large column were 24.3 cm i.d. × 25.1 cm length and 10.2 cm i.d. × 56.0 cm length, respectively. Two test columns were found necessary due to the wide range of bubble volume, bubble rise velocity, entrained volume and fluid properties tested in the experiments. The two columns were identical, however, in all functional aspects with the exception of the physical dimensions. In operation, the liquid–liquid interface would be adjusted to lie just below the plane formed by the junction of the two sections. A mechanical shutter was mounted just above the junction plane to collect the volume of the denser, lower liquid that would be entrained into the lighter, upper liquid by a rising bubble.

Air bubbles of varying sizes could be injected at the bottom of the glass column by means of a micrometer syringe and holding-cup mechanism. After initially purging the system, a metered volume of gas would be injected by the syringe into the inverted holding cup. When ready, the cup would be quickly turned upward, allowing the injected gas to rise through the liquid layers as a single bubble. The lower sections were sized in order to ensure that the bubbles achieved their terminal velocities prior to penetrating the junction of the two liquids. An inverted funnel with attached burette was mounted at the top of the test section, facing downwards, and submerged in the upper liquid. The rising gas bubble was intercepted by the funnel and trapped in the burette. In this fashion, the bubble volume could be precisely determined by measuring the volume of liquid displaced from the burette. The precision of this technique was $\pm 0.002\ \text{cm}^3$.

*Procedure*

In the experiments, a pair of immiscible liquids would be charged into the apparatus and adjusted to set the liquid–liquid interface at the junction of the two cylindrical sections. A specified volume of air would be injected into the holding cup, then allowed to rise as a single bubble through the two layers. Visual observations and video recordings would be made during the time of bubble transit and entrainment. The volume of the lower, heavy fluid that was entrained in the wake of the rising bubble would be intercepted by the mechanical shutter device. The shutter would be simply rotated in a horizontal, sweeping motion to cover the junction at the interface of the two liquids, capturing the entrained liquid volume as it once again settled. The bubble would continue to rise until trapped in the burette, at which point an accurate determination of the actual bubble volume could be made. The entrained droplets were recovered from the shutter plate, separated from the lighter liquid, and measured. All experiments, with the exception of those using R11 refrigerant, were performed at room temperature. Due to its low boiling point, the R11 fluid had to be refrigerated to 40–50°F to prevent vaporization during the tests. However, the properties of the R11 that were used in the data analysis were measured at this refrigerated temperature.

*Test fluids and ranges*

Table 1 lists the eight pairs of test fluids that were used in these experiments. The liquid properties were measured as a part of the test program. The properties listed were measured at the same temperature as the

Table 1. Test fluid properties†

| Fluid pair | Density (g cm$^{-3}$) | Viscosity (poise) | Surface tension (dyn cm$^{-1}$) | Interfacial tension (dyn cm$^{-1}$) |
|---|---|---|---|---|
| 10 cs silicone oil | 0.94 | 0.094 | 19.3 | 10.8 |
| Water (colored with $CuSO_4$) | 1.04 | 0.010 | ~70.0 | |
| 100 cs silicone oil | 0.97 | 0.97 | 20.6 | 31.1 |
| Water (colored with $CuSO_4$) | 1.01 | 0.010 | ~70.0 | |
| Water | 1.00 | 0.015 | 71.2 | 24.4 |
| R11 (40 50 F) | 1.48 | 0.0053 | 20.4 | |
| Water | 1.00 | 0.010 | 71.2 | 16.5 |
| Bromoform | 2.87 | 0.020 | 42.2 | |
| Hexane | 0.66 | 0.0033 | 18.4 | 2.4 |
| Water (colored with $CuSO_4$) | 1.00 | 0.010 | ~70.0 | |
| Glycerine | 1.26 | 14.9 | 63.1 | 14.0 |
| Bromoform | 2.87 | 0.020 | 42.2 | |
| Acetone | 0.81 | 0.0033 | 24.0 | 2.7 |
| Glycerine | 1.26 | 14.9 | 63.1 | |
| 100 cs silicone oil | 0.97 | 0.97 | 20.6 | 3.32 |
| Bromoform | 2.87 | 0.020 | 42.2 | |

† All fluid properties were measured or otherwise determined at 70 F with the exception of R11 refrigerant.

experiments. Densities were obtained by gravimetric measurements to a precision of $\pm 0.01$ g cm$^{-3}$ using a Mettler H51AR analytical balance. Surface tension and interfacial tension were measured to a precision of 0.05 dyn cm$^{-1}$ with a Fisher Surface Tensiomat (Model 21) which utilizes the duNouy ring method. The tabulated values are average values obtained from ten measurements for each fluid. It should be mentioned that surface tension and interfacial tension are sensitive to small amounts of impurities or additives (e.g. copper sulfate used to color the water), and direct measurements of these transport properties had to be obtained with the actual test fluids. Kinematic viscosity was measured with appropriately sized Cannon–Ubbelohde capillary tube viscometers with negligible uncertainty. The two silicone oils used in this investigation were tested in the Irvine–Park Falling Needle Viscometer to determine their viscosities and verify their Newtonian behavior. The glycerine used in these studies was USP White Glycerine (CAS #56-81-5); measurement of its viscosity was beyond the capability of our instrumentation. The value quoted in Table 1 is from ref. [16].

*Bubble rise velocity*

It was necessary to know the bubble rise velocities for these tests in order to calculate the bubble Reynolds number. No theory was found which would accurately and reliably predict the bubble rise velocity in any fluid other than water. Therefore, the bubble terminal rise velocities were measured for air bubbles in each of the test fluids as part of the experimental program. A separate cylindrical test column was constructed into which the bubble holding-cup mechanism could be installed. Bubbles, which covered the size range used in the entrainment experiments, were released and their time-of-flight was timed over two separate courses in their ascent. It was required that the velocities over both courses be identical in order for it to be considered at terminal velocity. The terminal velocities indicated in Fig. 3 represent the average of 20 runs for each bubble size tested.

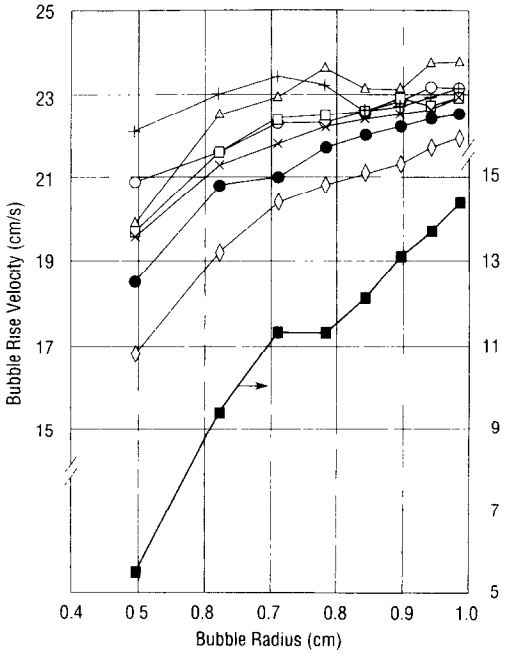


FIG. 3. Measured bubble rise velocities: +, water; ○, acetone; △, R11; □, hexane; ×, 10 cs silicone oil; ●, bromoform; ◇, 100 cs silicone oil; ■, glycerine.

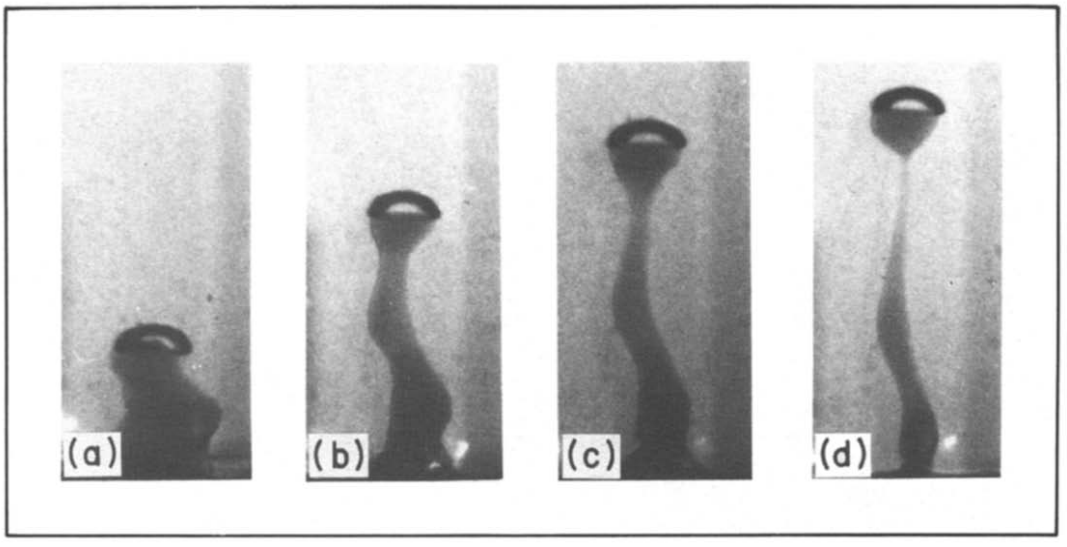


FIG. 4. Photograph of entrainment phenomenon.

## RESULTS

This section presents sample experimental results and discusses their implications.

*Observations of phenomenon*

Figure 4 shows a series of frames from a high-speed photographic record of a single discrete bubble rising through the stratified liquid layers. During this series of frames, the gas bubble has passed into the upper pool and a volume of the denser liquid is clearly seen to be entrained in its wake, having been pulled through the interface between the two liquid layers. Studies of the high-speed movies showed that entrainment starts when a gas bubble of sufficient volume penetrates the surface and pulls a column of the lower liquid in its wake into the upper pool. If the bubble volume is of insufficient size, the levitated column falls back to the lower pool and the gas bubble continues to rise through the upper pool without having caused any entrainment. For sufficiently large gas bubbles, the levitated column rises to a sufficient height that it becomes hydrodynamically unstable; as it elongates, it necks down to snap free a glob of the denser fluid which is then considered to be successfully entrained into the upper fluid layer. Our experiment permitted the capture and measurement of the volume of such entrained globules. Observations of the phenomena from the visual recordings indicated that the volume of entrainment would be affected not only by the size of the gas bubble but also by the densities of the two liquid fluids, their viscosities, and the interfacial tension between the two liquids. Experimental indications of these parametric effects are described below.

*Effect of heavy-liquid density*

Figure 5 shows the experimental data indicating volumes of entrained liquid for individual bubbles of various sizes (volumes). Results are plotted for two pairs of fluids, water overlying R11 and water overlying bromoform. The major parametric difference between these two pairs is the density of the heavier liquid, bromoform being 2.9 times more dense than water. It is seen that the entrainment volume for a given bubble volume decreased very significantly with increasing density of the heavy liquid, the water/bromoform entrainment volumes being almost an order of magnitude lower than the corresponding entrainment volumes for water/R11.

*Effect of light-liquid density*

The effect of the light-liquid density is just the opposite. Figure 6 shows data for two pairs of fluids, silicone oil over water and hexane over water. The major parametric difference between these two pairs

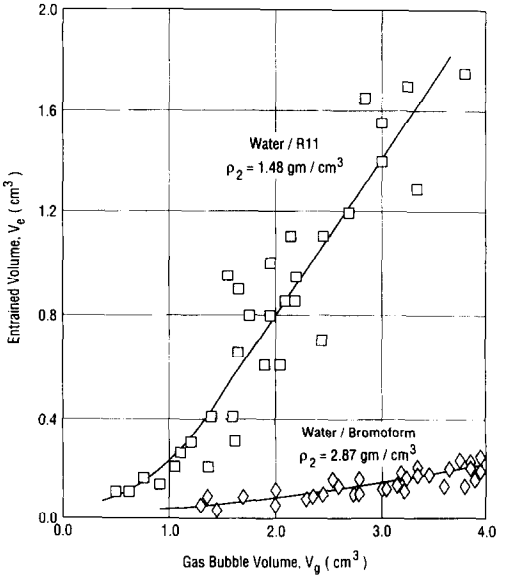


FIG. 5. Effect of heavy-liquid density.

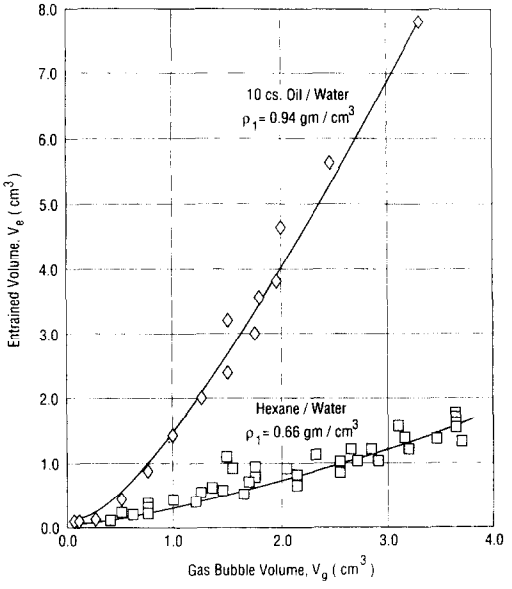


FIG. 6. Effect of light-liquid density.

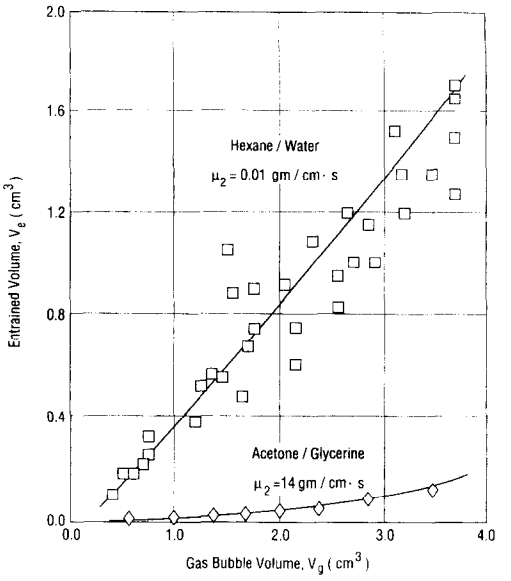


FIG. 8. Effect of heavy-liquid viscosity.

is the density of the upper layer light fluid, hexane, with a specific density of 0.7 as compared to silicone oil with a specific density of 0.9. These results clearly show that entrainment volumes increased with increasing density of the light liquid. For the fluids indicated, a density ratio of 1.5 in the upper layer fluid resulted in a factor of approximately four in the entrainment volumes, for the same bubble volume. Combined with the observations of Fig. 5, the experimental results demonstrate the importance of buoyancy difference between the two liquids.

*Effect of interfacial tension*

Figure 7 shows measurements obtained with the two pairs of fluids, water over R11 and hexane over water. Both of these pairs have a relative density difference of approximately 0.4 g cm$^{-3}$ between the heavier and lighter liquids so that relative buoyancy should not be a factor. The major parametric difference between these two pairs is the interfacial tension ($\sigma_{12}$) which differed by almost a factor of ten. The results plotted in Fig. 6 show that there is little discernible difference in the entrainment volumes between these two pairs of fluids. However, the minimum gas bubble volumes for which measurable entrainment could be obtained was found to be 0.03 cm$^3$ for water over R11 and 0.002 cm$^3$ for hexane over water. The conclusion from this observation is that the interfacial tension affected the onset of entrainment but has relatively small effect on the volume of entrainment. The first effect is consistent with the results reported in ref. [3].

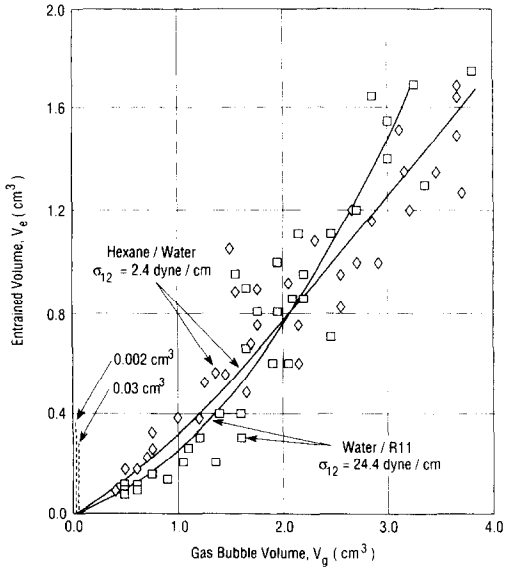


FIG. 7. Effect of interfacial surface tension.

*Effect of heavy-liquid viscosity*

While the liquid viscosities do not affect static force balances, they would be expected to affect bubble rise velocities which in turn influence the characteristics of the bubble wake. Figure 8 examines the potential effect of the liquid viscosity of the heavier liquid in the lower pool. The two pairs of fluids illustrated in this figure have essentially identical viscosities in the lighter fluid and also similar density differences; the major parametric dependence is in the viscosity of the heavy liquids which differ by a factor of over 1000 for water and glycerine. The experimental results show a strong influence on the entrainment volumes. The low viscosity case (hexane/water) had entrainment volumes greater than 10 times that of the high viscosity case (acetone/glycerine).

*Effect of light-liquid viscosity*

Figure 9 illustrates the effect of different viscosities for the light liquids in the upper pool. Data are plotted

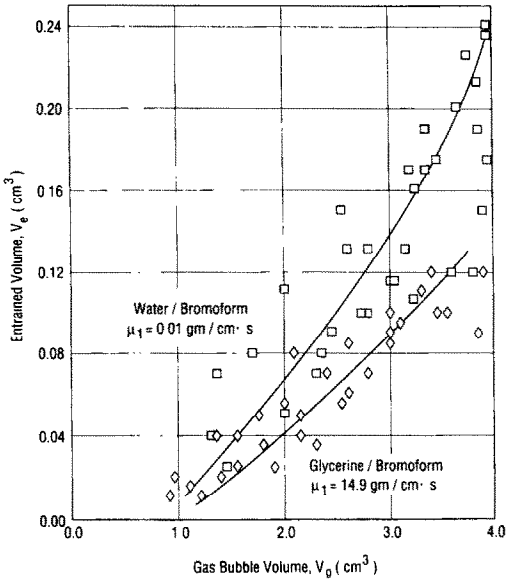


FIG. 9. Effect of light-liquid viscosity.

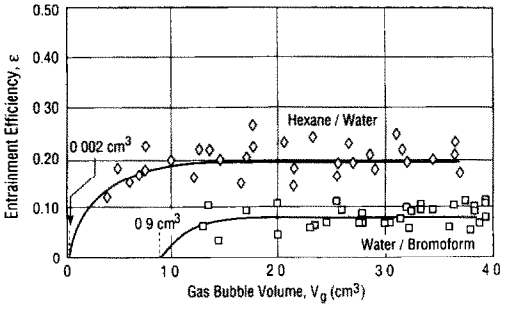


FIG. 10. Examples of entrainment efficiencies.

for water over bromoform and glycerine over bromoform. These two pairs of test fluids had the same heavier liquid (bromoform) and similar buoyancy density differences. Thus this figure illustrates the parametric effect of the upper fluid (light liquid) viscosity. It is seen that while there is a discernible increase in entrainment volume for the less viscous case, the magnitude of the effect for changing light-liquid viscosity is much less than that for changing viscosity of the heavy liquid.

## CORRELATION

The experimental results clearly indicate that the volume of entrainment from the lower pool into the upper pool by a discrete gas bubble is a function of the gas bubble volume, the densities of the two liquids, the viscosity of the two liquids, and the interfacial tension between the two liquids. Over the range of experimental tests for eight different fluid pairs, the resultant entrainment volume per bubble varied over two orders of magnitude. The development of a correlation to represent this experimental data base is presented here.

It was first noted that, for a given pair of liquids, entrainment would be possible by discrete gas bubbles only if the bubble volume exceeded the criterion for onset presented in ref. [3]

$$V_g \geqslant V_{go}. \tag{1}$$

$V_{go}$ was theoretically derived in ref. [3], and is given by

$$V_{go} = \left[\frac{7.8\sigma_{12}}{g(3\rho_1 - \rho_2 - 2\rho_g)}\right]^{3/2}. \tag{2}$$

A static force balance was constructed (assuming negligible inertial forces) to determine the maximum theoretical liquid volume that could be entrained across the liquid–liquid interface by a rising gas bubble which exceeds this entrainment onset volume. As the bubble (in this analysis the bubble is assumed to be a spherical cap) rises across the liquid–liquid interface, it is observed that a column of the lower, heavy fluid rises with it due to buoyancy and wake effects associated with the bubble. We will consider a control volume consisting of the rising gas bubble and the levitated column of the lower, heavy liquid. By considering the upward lifting force due to the buoyancy of the bubble on the column of entraining fluid, the restoring force on the fluid column due to interfacial tension with the upper fluid, and negative buoyancy of the entrained column in the upper layer, the following force balance was derived:

$$(\rho_1 - \rho_g)gV_g = 2\pi\left(\frac{3V_g}{2\pi}\right)^{1/3}\sigma_{12} + V_{m,e}(\rho_2 - \rho_1)g. \tag{3}$$

The first term is due to bubble buoyancy, the second term represents the effect of interfacial tension as the levitated column attempts to tear free from the lower layer, and the third term is the restoring buoyancy of the entraining column. This can be rearranged to solve for the maximum volume of lower liquid ($V_{m,e}$) that can be levitated into the lighter upper liquid as follows:

$$V_{m,e} = \frac{V_g(\rho_1 - \rho_g) - (\sigma_{12}/g)(12\pi^2 V_g)^{1/3}}{(\rho_2 - \rho_1)}. \tag{4}$$

One can consider an 'efficiency' of entrainment ($\varepsilon$) by taking the ratio of actual entrainment volume ($V_e$) to the maximum entrainable volume ($V_{m,e}$)

$$\varepsilon = \frac{V_e}{V_{m,e}}. \tag{5}$$

Figure 10 shows plots of the experimentally obtained entrainment efficiencies vs the gas bubble volume, for two sample liquid pairs. It is seen that for a given pair of fluids, $\varepsilon$ initially increases rapidly when $V_g$ exceeds $V_{go}$, but then seems to approach asymptotic limits at higher values of $V_g$. For the cases tested, the entrainment efficiency varied over two orders of magnitude but did not exceed 0.3. Other pairs of test fluids pre-

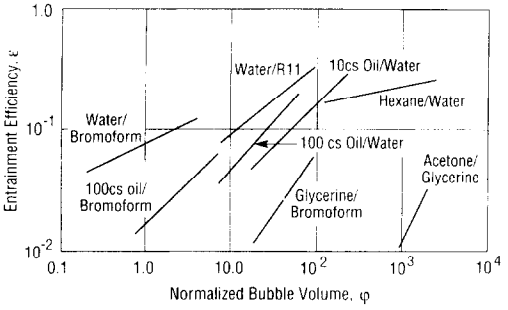


FIG. 11. Variation of entrainment efficiency with normalized bubble volume.

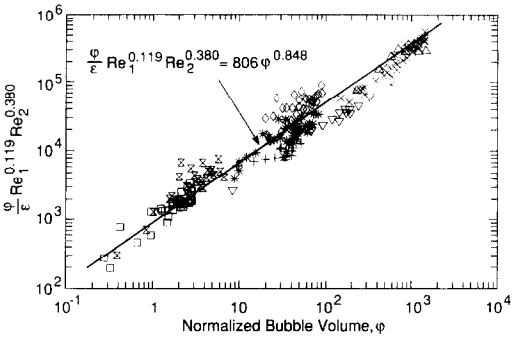


FIG. 12. Correlation of data: □, water/bromoform; ⊠, 100 cs silicone oil/bromoform; ▽, 10 cs silicone oil/water; *, water/R11; +, 100 cs silicone oil/water; ◇, glycerine/bromoform; △, acetone/glycerine; ×, hexane/water.

sented parametric curves similar to those plotted in Fig. 10.

A normalized driving force for entrainment can be defined, based on the excess bubble volume beyond that required to cause onset of entrainment, as

$$\phi = \frac{V_g - V_{go}}{V_{go}}. \tag{6}$$

When the entrainment efficiencies are plotted vs $\phi$, approximately linear line segments are obtained on log–log coordinates, as shown in Fig. 11. Parametric variations in the magnitude of $\varepsilon$ are obviously related to the fluid properties of the stratified liquid layers.

As indicated above, photographic observations had indicated that entrainment occurs by capturing a volume of the dense liquid in the wake, as the gas bubble passes through the liquid–liquid interface.

It seems reasonable to expect that any inefficiency in the entrainment process would be associated with the size and character of the bubble wakes. The bubble wakes are in turn affected by bubble diameter and velocity, the fluid viscosity, and density. These parameters are conveniently grouped in the bubble Reynolds number

$$Re_1 = \frac{\rho_1 u_{b1} d_b}{\mu_1} \quad \text{for lighter liquid}$$

$$Re_2 = \frac{\rho_2 u_{b2} d_b}{\mu_2} \quad \text{for denser liquid} \tag{7}$$

where $d_b$ is taken to be the bubble diameter for an equivalent spherical volume of gas. In this investigation, the terminal rise velocities ($u_{b1}$, $u_{b2}$) were experimentally determined as a function of the gas volume ($V_g$) for each fluid. In situations when experimental determination is not possible, published correlations can be used [17].

Following this reasoning, a functional relationship of the form

$$\varepsilon = f(\phi, Re_1, Re_2)$$

was sought. The final correlation was represented as

$$\frac{\phi}{\varepsilon}(Re_1)^a(Re_2)^b = K\phi^c \tag{8}$$

where the constants were empirically determined to be

$$a = 0.119$$

$$b = 0.380$$

$$c = 0.848$$

$$K = 806.$$

Figure 12 shows a graphical comparison of this correlation with all the experimental data obtained in this investigation. The statistical fit corresponds to a mean deviation of 0.35 in the ratio of measured to calculated entrainment efficiency.

## SUMMARY

The process of liquid entrainment between stratified liquid layers by rising gas bubbles was experimentally investigated for eight different pairs of liquids, covering a wide range of physical properties. In addition to photographic observations, quantitative measurements of the entrained liquid volumes were obtained for a range of gas bubble sizes. The results indicated that once the gas bubble exceeded the necessary minimum size to cause onset of entrainment, measurable entrainment occurred which increased with excess gas volume (above the required onset volume). The efficiency of entrainment, defined as the ratio of entrained volume to maximum entrainable volume as derived from a limiting static force balance, was found to range over two orders of magnitude but did not exceed 0.3 for any of the test cases. A dimensionless correlation was obtained to represent the entrainment efficiency as a function of the excess gas volume ($\phi$), and the gas bubble Reynolds numbers in each liquid ($Re_1$, $Re_2$). Agreement between the proposed correlation and the 189 experimental data points indicated a mean deviation of 0.35.

*Acknowledgements*—The authors would like to acknowledge the technical assistance of Mr Charles Finfrock who assisted in the design and construction of the experimental apparatus, selection of the test fluids and measurements of their physical

properties, and execution of the experiments. The skilful preparation of the manuscript by K. Becker, L. Hanlon and N. Siemon is gratefully acknowledged. This work was performed under the auspices of the United States Nuclear Regulatory Commission, and the support of the staff, especially Dr S. B. Burson, is gratefully acknowledged.

## REFERENCES

1. J. Szekely, Mathematical model for heat or mass transfer at the bubble-stirred interface of two immiscible liquids, *Int. J. Heat Mass Transfer* **6**, 417–422 (1963).
2. G. A. Greene and T. F. Irvine, Jr., Heat transfer between stratified immiscible liquid layers driven by gas bubbling across the interface, *1988 Natn. Heat Transfer Conf., ANS Proc.*, HTC-Vol. 3, pp. 31–36 (1988).
3. G. A. Greene, J. C. Chen and M. T. Conlin, Onset of entrainment between immiscible liquid layers due to rising gas bubbles, *Int. J. Heat Mass Transfer* **31**, 1309–1317 (1988).
4. J. L. Mercier, F. M. da Cunha, J. T. Teixeira and M. P. Scofield, Influence of enveloping water layer on the rise of air bubbles in Newtonian fluids, *J. Appl. Mech.* **96**, 29–34 (1974).
5. Y. H. Mori, K. Komotori, K. Higeta and J. Inada, Rising behavior of air bubbles in superposed liquid layers, *Can. J. Chem. Engng* **55**, 9–12 (1977).
6. M. Epstein, D. J. Petrie, J. H. Linehan, G. A. Lambert and D. M. Cho, Incipient stratification and mixing in aeratcd liquid–liquid or liquid–solid mixtures, *Chem. Engng Sci.* **36**, 784–787 (1981).
7. A. Suter and G. Yadigaroglu, Bubble-driven mixing of the oxidic and metallic phases during MCCI, *Trans. Am. Nucl. Soc.* **56**, 401–403 (1988).
8. D. Poggi, R. Minto and W. G. Davenport, Mechanisms of metal entrapment in slag, *J. Metals* **21**, 40–45 (1969).
9. F. B. Cheung, G. Leinweber and D. R. Pedersen, Bubble-induced mixing of two horizontal liquid layers with non-uniform gas injection at the bottom, *Proc. Sixth Inf. Exchange Meeting on Debris Coolability*, EPRI NP-4455 (1986).
10. M. Veeraburus and W. O. Philbrook, Observations on liquid–liquid mass transfer with bubble stirring. In *Physical Chemistry of Process Metallurgy*. Interscience, New York (1959).
11. F. Gonzalez and M. Corradini, Experimental study of pool entrainment and mixing between two immiscible liquids with gas injection, OECD–CSNI Workshop on Core Debris/Concrete Interactions, Palo Alto, California (1986).
12. G. A. Greene, C. E. Schwarz, J. Klages and J. Klein, Heat transfer between immiscible liquids enhanced by gas bubbling, Int. Meeting on Thermal Nuclear Reactor Safety, Chicago, Illinois (1982).
13. G. A. Greene and C. E. Schwarz, An approximate model for calculating overall heat transfer between overlying immiscible liquid layers with bubble-induced liquid entrainment, Information Exchange Meeting on Post Accident Debris Cooling, Karlsruhe, F.R.G. (1982).
14. H. Werle, Enhancement of heat transfer between two horizontal liquid layers by gas injection at the bottom, *Nucl. Technol.* **59**, 160–164 (1982).
15. A. J. Suo-Anttila, The mixing of immiscible liquid layers by gas bubbling, NUREG/CR-5219 (1988).
16. *Lange's Handbook of Chemistry* (Edited by J. A. Dean), 12th Edn, pp. 10–97. McGraw-Hill, New York (1979).
17. G. B. Wallis, *One-dimensional Two-phase Flow*. McGraw-Hill, New York (1969).

## ENTRAINEMENT INDUIT PAR UNE BULLE ENTRE DES COUCHES LIQUIDES STRATIFIEES

**Résumé**—On considère expérimentalement le phénomène d'entrainement liquide par une bulle de gaz qui s'élève verticalement à travers l'interface entre deux couches liquides immiscibles. On développe ensuite un modèle analytique/empirique qui prédit le volume de liquide entrainé, en fonction du volume de la bulle, des propriétés physiques et de transport des deux liquides. L'efficacité de l'entrainement est présentée en fonction du volume réduit de bulle et des nombres de Reynolds dans chaque fluide. Le calcul et les résultats expérimentaux s'accordent bien pour lés huit paires de liquides non miscibles.

## BLASENINDUZIERTES ENTRAINMENT IN GESCHICHTETEN FLÜSSIGKEITEN

**Zusammenfassung**—In dieser vorwiegend experimentellen Arbeit wird das Flüssigkeits-Entrainment untersucht, das durch eine vertikal aufsteigende Gasblase an der Grenzfläche zwischen zwei nicht-mischbaren Flüssigkeitsschichten verursacht wird. Ein analytisch/empirisches Modell wird entwickelt, welches das Volumen des Flüssigkeits-Entrainments als Funktion des Blasenvolumens, der physikalischen Stoffwerte und der Transportgrößen der beiden Flüssigkeiten berechnet. Der Entrainment-Wirkungsgrad wird als Funktion des reduzierten Blasenvolumens und der Blasen-Reynolds-Zahl in jeder Flüssigkeit dargestellt. Der Vergleich mit experimentellen Daten von acht nicht-mischbaren Flüssigkeitspaaren zeigt gute Übereinstimmung.

## УНОС ЖИДКОСТИ ПУЗЫРЬКАМИ ГАЗА ПРИ ПОДЪЕМЕ В СТРАТИФИЦИРОВАННЫХ СЛОЯХ ЖИДКОСТИ

**Аннотация**—Экспериментально исследуется явление уноса жидкости пузырьком газа, поднимающимся вертикально у границы раздела двух несмешивающихся жидких слоев. Разработана полуэмпирическая модель для расчета объема уносимой жидкости в зависимости от объема пузырьков, а также от физических свойств и характеристик переноса двух жидкостей. Эффективность уноса представлена как функция приведенного объема пузырьков и чисел Рейнольдса для пузырьков в каждой жидкости. Обобщенное соотношение и полученные результаты хорошо согласуются с экспериментальными данными для восьми пар несмешивающихся жидкостей.